



# OPEN Effect of pH on the surface charges of permanently/variably charged soils and clay minerals

Hua Cao, Xinmin Liu, Bo Feng, Jiaqi Sun, Deyuan Ma, Xijing Chen & Hang Li✉

Traditionally, the surface charge number (SCN) of permanently charged soils/clay minerals is believed to be unaffected by environmental pH. However, recent studies have revealed the occurrence of polarization-induced covalent bonding between  $H^+$  and the surface O atoms of permanently charged clay minerals. This discovery challenges the traditional notions of “permanently charged soil” and “permanently charged clay mineral”. The purpose of this study is to confirm that there are no true “permanently charged clay” or “permanently charged soil”. In this study, the SCNs of two permanently charged clay minerals, two variably charged clay minerals, five permanently charged soils (temperate soils), and four variably charged soils (tropical or subtropical soils) were measured at different pH values using the universal determination method of SCN. The results showed that: (1) The SCNs of the permanently/variably charged soils and clay minerals decreased significantly with decreasing pH; (2) the SCN of montmorillonite decreased less with decreasing pH than the SCNs of variably charged minerals, whereas the SCN of illite decreased to nearly the same extent, indicating strong polarization-induced covalent bonding between  $H^+$  and the surface O atoms of illite; (3) the SCNs of permanently charged soils decreased to a similar extent as those of variably charged soils with decreasing pH. This study demonstrated that the concepts, “permanently charged clay mineral” or “permanently charged soil”, are questionable because of the polarization-induced covalent bonding between  $H^+$  and the surface O atoms of clay minerals.

**Keywords** Asymmetric hybridization orbitals, Surface charge number, Permanent charge, Variable charge, Polarization-induced covalent bonding

The surface charge number (SCN) is one of the most significant characteristics in soil colloid and interface science. Considering that most electrochemical reactions occur on clay particle surfaces, the research on SCN is very important for understanding and elucidating various physicochemical phenomena in soil<sup>1–3</sup>. SCN determines the number of ions that can be adsorbed by soil, and the surface charge density plays a key role in the strength of adsorption of these ions<sup>4</sup>. The electrostatic force generated by the surface charge serves as a significant driving force for a range of interfacial reactions<sup>5,6</sup>. For instance, when  $NH_4^+$  is applied to soil, it is adsorbed around soil particles through electrostatic attraction. The electric field surrounding soil particles determines the strength of the electrostatic attraction of  $NH_4^+$ , which in turn impacts the nitrification rate<sup>7</sup>. The leaching of  $NO_3^-$  resulting from nitrification is also influenced by the strength of electrostatic repulsion. The  $H^+$  produced during nitrification readily displaces base cations (e.g.,  $Ca^{2+}$  and  $Mg^{2+}$ ) on clay particle surface. Consequently, the leaching of  $NO_3^-$  inevitably leads to the coupled migration of base ions due to principle of electrical neutrality, resulting in accumulation of  $H^+$  and a decrease in base cations on soil particle surface. This is the microscopic mechanisms of well-known soil acidification<sup>8</sup>. Clay minerals often exhibit high SCN, such as zeolite, with a microporous structure; montmorillonite, with expansibility; and mica, with a layered structure<sup>9–11</sup>. This characteristic imparts significant application value to these materials in the remediation of heavy metal-contaminated soil<sup>12,13</sup>.

Schofield<sup>14</sup> first introduced the concepts of “permanent charge” and “variable charge” in soil, suggesting that the charges carried by soil can be categorized into two parts. One part represents the nature of clay minerals and remains permanent regardless of environmental pH, which is well known as permanent charge. The other part consists of the surface charges that varies with pH, which is termed variable charge. It is widely acknowledged that the amount of permanent negative charges generated by isomorphous substitution does not change with environmental pH. 2:1 clay minerals such as montmorillonite, illite, and vermiculite are common permanently

Chongqing Key Laboratory of Soil Multi-Scale Interfacial Process, College of Resources and Environment, Southwest University, Chongqing 400715, China. ✉email: lihangswu@163.com

charged clay minerals. In variably charged soils, the primary sources of variable charges stem from oxides and hydrated oxides of iron and aluminum<sup>4</sup>. Based on the nature of surface charges, soils can be classified into two categories: permanently charged soil (temperate soil) and variably charged soil (tropical or subtropical soil)<sup>4,15</sup>. Permanently charged soils are typically found in temperate regions and are characterized by a mineral composition dominated by 2:1 phyllosilicate<sup>16</sup>. In contrast, variably charged soils, which are more prevalent in tropical or subtropical regions, exhibit higher levels of iron and aluminum oxides<sup>17,18</sup>.

The surface O atoms of clay minerals (such as montmorillonite and illite) are Lewis soft bases. It suggests that the lone pair electrons of surface O atoms have low activity, making it difficult for them to form stable coordination bonds with H<sup>+</sup><sup>19</sup>. However, Sposito<sup>19</sup> also proposed that the electric field generated by the negative charges of clay minerals can activate the lone pair electrons of surface O atoms. In particular, the electrostatic field strength of tetrahedrally substituted illite was found to be stronger than that of octahedrally substituted montmorillonite, resulting in more active lone pair electrons of the surface O atoms of illite and the formation of relatively strong inner-sphere surface complexes<sup>20</sup>. The assertion made by Sposito has been recently verified. Recent studies<sup>6,21</sup> have revealed that the asymmetric hybridization of the outer shell orbitals of surface O atoms occurs under an asymmetric electric field at soil particle surface. It results in a notable alteration in the energy levels of the outer shell orbitals of surface O atoms, consequently intensifying the reactivity of the lone pair electrons of surface O atoms. The correlations between the 2s2p orbital/energy and the classical orbital/energy of surface O atoms in charged clay minerals are as follows:

$$\begin{aligned}\phi_{(1)} &= \frac{1}{\sqrt{2}} [\psi_{2s} + \psi_{2p_z(-)}], & E_1^2 &= E_{20} + 3e\xi \frac{a_0}{(1-a)Z} \\ \phi_{(2)} &= \frac{1}{\sqrt{2}} [\psi_{2s} + \psi_{2p_z(+)}], & E_2^2 &= E_{20} - 3e\xi \frac{a_0}{(1-a)Z} \\ \phi_{(3)} &= \psi_{2p_x}, & E_3^2 &= E_{20} \\ \phi_{(4)} &= \psi_{2p_y}, & E_4^2 &= E_{20}\end{aligned}$$

where  $\xi$  is electric field strength at surface;  $\psi$  is classic 2s2p orbital of surface O atom as  $\xi = 0$ , and  $E_{20}$  is the energy of the orbital;  $\phi$  is the 2s2p orbital of surface O atom of charged clay minerals, and  $E_2^1$  is the energy of the orbital;  $a_0$  is Bohr radius;  $\alpha = S/Z$ , S is shielding constant and Z is nuclear charge number of O atom.

According to the above wave function  $\phi$ , the variation in the 2s2p orbitals of the surface O atoms of charged clay minerals is illustrated in Fig. 1<sup>16</sup>. The figure indicates that the 2s2p orbitals of the surface O atoms of charged clay minerals in the z direction are indeed activated.

Li et al.<sup>22</sup> corroborated through ion adsorption kinetics, adsorption energy measurements, critical coagulation concentration analysis of colloid aggregation, and infrared spectroscopy that the Lewis acid-base reaction between surface O atoms and Cu<sup>2+</sup>/Ca<sup>2+</sup>/Mg<sup>2+</sup>/H<sub>2</sub>O was significantly enhanced by the asymmetric hybridization of the surface O atoms in an electric field. Furthermore, Liu et al.<sup>6</sup> discovered that the nonelectrostatic adsorption energy of H<sup>+</sup> on clay mineral surfaces stemmed from the coordinate bonding between H<sup>+</sup> and surface O atoms. Notably, the adsorption energy of H<sup>+</sup> was influenced by electrostatic field strength. A study conducted by Liu et al.<sup>5</sup> revealed that, in addition to electrostatic adsorption, polarization-induced covalent adsorption of H<sup>+</sup> on the montmorillonite surface occurred. Moreover, the polarization-induced covalent adsorption energy of

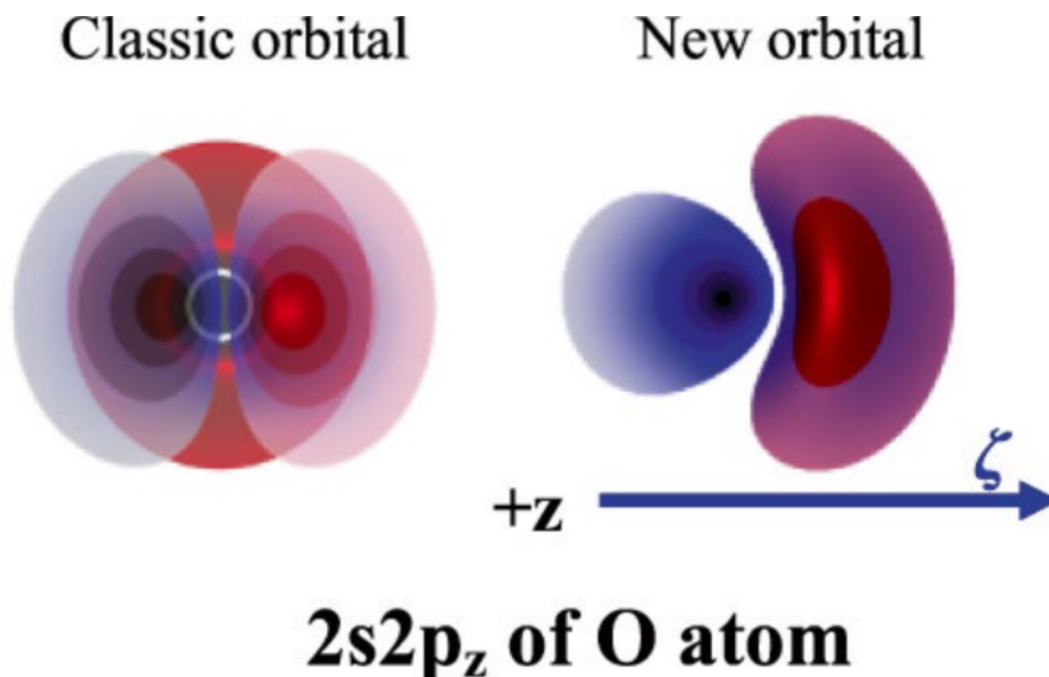


**Fig. 1.** The variation in the 2s2p orbitals of the surface O atoms of charged clay minerals in an electric field.

$H^+$  increased linearly with increasing electrostatic field strength, which was in accordance with the quantum mechanical analysis of the asymmetric hybridization orbitals of the surface O atoms of montmorillonite.

Given that the polarization-induced covalent adsorption of  $H^+$  on clay mineral surfaces results in an increase in the positive surface charges or a decrease in the negative surface charges, it is imperative to acknowledge that pH exerts a significant influence on soil SCN. In this case, there is a risk that the SCN in a permanently charged soil will decrease in the face of acidification, which will undoubtedly have an impact on soil productivity. Consequently, the objectives of this study are to investigate the impact of pH on the SCNs of permanently/variably charged clay minerals and soils.

## Materials and methods

### Experimental materials

The montmorillonite and kaolinite used in this study were purchased from Wu Hua Tian Bao Mineral Resources Co., Ltd., Inner Mongolia, China, and the illite was purchased from Shan Lin Shi Yu Mineral Products Co., Ltd., Guizhou, China. Goethite was synthesized through the following procedures<sup>23</sup>. First, 200 g of  $Fe(NO_3)_3 \cdot 9H_2O$  was added to 3300 mL of ultrapure water, and then, 320 mL of 5 mol/L NaOH solution was added dropwise at a rate of 5 mL/min until the pH of the final solution surpassed 12. During this process, the mixture was continuously stirred using a glass rod. The resulting suspension was then incubated in an oven at 333 K for 48 h. After the aging period, the supernatant was discarded through centrifugation. The precipitate was washed with ultrapure water until the conductivity of the supernatant decreased to less than 20  $\mu S/cm$ . Finally, the washed precipitate was dried at 343 K, crushed, and sieved through a 0.25 mm mesh for further experiments.

The black soil (Mollisol) was collected from Suihua, Heilongjiang (46°57' N, 125°58' E); the chernozem (Mollisol) and chestnut soil (Mollisol) were collected from Hulunbuir, Inner Mongolia (50°21' N, 120°22' E; 50°00' N, 119°10' E); the dark brown soil (Alfisol) was collected from Jilin, Jilin (43°55' N, 126°09' E); the brown soil (Alfisol) was collected from Yantai, Shandong (36°94' N, 120°60' E); the yellow-brown soil (Alfisol) was collected from Nanjing, Jiangsu (31°17' N, 118°40' E); the yellow soil (Alfisol) was collected from Beibei, Chongqing (29°80' N, 106°40' E); the red soil (Ultisol) was collected from Yingtan, Jiangxi (27°44' N, 116°48' E); and the latosol (Ultisol) was collected from Danzhou, Hainan (19°50' N, 109°49' E). The soil samples were taken from a depth of 0–20 cm within the soil profile, with care taken to remove plant roots, stones, and other debris. The samples were then dried at room temperature, ground into a fine powder, and sieved through a 2 mm mesh for further analysis. The basic properties of the studied soils are presented in Table 1.

Soil pH was determined in a suspension with soil/solution ratio of 1:2.5 (w: v), using a pH meter with a pH electrode (E201F, INESA Scientific instrument co., Ltd. China). Soil electrical conductivity (EC) was determined in a suspension with soil/solution ratio of 1:5 (w: v), using an EC meter (DDS-307 A, INESA Scientific instrument co., Ltd. China). Soil organic matter was determined using the dichromate method.

Soil clay particles ( $< 2 \mu m$ ) were separated by the pipette method and subsequently analyzed for clay mineral composition via X-ray diffraction (XRD) (XD-3, Persee, Beijing, China, Cu  $K\alpha$ -R, diffraction angles = 5°–40°, step value = 2°/min). The XRD profiles of the soil samples were analyzed with MDI Jade 6.0 software. The relative contents of clay minerals were calculated based on the diffraction peak areas of the XRD profiles<sup>24</sup>.

### SCN determination experiments

In the SCN determination experiments,  $H^+$ -saturated samples were needed. For example, the  $H^+$ -saturated montmorillonite sample was prepared as follows: Fifty grams of montmorillonite powder was weighed into a 1000 mL triangle bottle and washed successively by dispersion, centrifugation, and decantation with three portions of 0.1 mol/L HCl solution and then three portions of ultrapure water. Following the final decantation of the supernatant, the  $H^+$ -saturated montmorillonite was dried at 343 K, crushed, and sieved through a 0.25 mm mesh for subsequent experiments.

The SCNs of the clay minerals and soils were determined using the universal determination method of SCN, which was developed based on the new principles of interface atomic orbital asymmetric hybridization theory. According to it, the soil siloxane surface and the hydroxylated surface are initially transformed into  $[\equiv Si-O]-H^+$  and  $-OH^+$ , respectively. Subsequently, NaOH is added, and the suspension pH is adjusted through a swift “surface acid-base reaction”. It rapidly converts  $[\equiv Si-O]-H^+$  to  $[\equiv Si-O]^-$  and  $-OH^+$  to  $-OH$  or  $-O^-$ , with the

Soil type		pH	Organic matter g/kg	EC $\mu S/cm$
Permanently charged soils	Black soil	6.54	46.0	180
	Chernozem	7.40	115	297
	Chestnut soil	6.57	46.7	52.1
	Dark brown soil	6.02	11.7	34.9
	Brown soil	5.22	11.6	83.2
Variably charged soils	Yellow-brown soil	5.58	19.6	209
	Yellow soil	5.47	10.8	24.1
	Red soil	4.76	10.1	125
	Latosol	4.94	7.78	30.1

**Table 1.** Basic properties of the studied soils.

amount of conversion being controlled by the pH. The released negative charges are balanced by  $\text{Na}^+$ . According to asymmetric hybridization orbital theory, the observed adsorption energy of  $\text{Na}^+$  can be attributed primarily to classic electrostatic interactions.

The universal determination method of SCN required the following steps. Initially, the  $\text{H}^+$ -saturated sample (the mass used was determined according to the SCN of the sample) was treated with 50 mL of 0.01 mol/L NaOH solution. After stirring, 0.5 mol/L AcOH solution was added to the suspension until it reached a pH of approximately 11. Subsequently, the  $\text{Na}^+$  activity in the suspension was determined by a  $\text{Na}^+$ -selective electrode (701, INESA Scientific instrument co., Ltd. China). 0.5 mol/L AcOH solution was added to adjust the pH in the suspension to a set value, and the  $\text{Na}^+$  activity in the suspension was again determined using the  $\text{Na}^+$ -selective electrode. Based on the measured activity, the  $\text{Na}^+$  concentration was subsequently calculated via the “iterative method”<sup>25</sup>. The surface charge at a set pH was calculated based on the amount of  $\text{Na}^+$  adsorbed, which was obtained by calculating the difference between the initial and equilibrium  $\text{Na}^+$  concentrations. By further adjusting the suspension's pH with additional 0.5 mol/L AcOH solution, the SCN at the corresponding pH was obtained according to the above procedures, thereby establishing a quantitative relationship between SCN and pH.

Importantly, during the determination of SCN at different pH values, specific standard solutions were used to calibrate the  $\text{Na}^+$ -selective electrode. For SCN determination at pH values between 5 and 11, the electrode was calibrated using 0.001, 0.01, and 0.1 mol/L NaCl solutions. However, when determining the SCN at pH 3, 4, and 5, the calibration process employed a broader concentration range of NaCl solutions at pH 3, 4, and 5, respectively, each including 0.001, 0.005, 0.01, 0.05, and 0.1 mol/L NaCl.

The SCNs of two permanently charged clay minerals (montmorillonite and illite), two variably charged clay minerals (kaolinite and goethite), five permanently charged soils (black soil, chernozem, chestnut soil, dark brown soil, and brown soil) and four variably charged soils (yellow-brown soil, yellow soil, red soil, and latosol) at different pH values were determined.

## Results

### Effects of pH on the SCNs of different clay minerals

The effects of pH on the SCNs of different clay minerals are shown in Fig. 2. The results of repeated experiments can be seen in Fig. S1 of the Supplementary Material. The negative surface charges of goethite gradually decrease with decreasing pH (Fig. 2a). Specifically, when the pH is approximately 7.80, the negative charges decrease to 0 cmol/kg, beyond which point the positive surface charges start to increase incrementally. With decreasing pH, the SCNs of montmorillonite, illite, and kaolinite gradually decrease. In terms of SCNs at the different pH values, the clay minerals follow the order montmorillonite > illite > kaolinite. For instance, at pH approximately 11, the SCNs of montmorillonite, illite, and kaolinite are  $-105$ ,  $-11.9$ , and  $-6.54$  cmol/kg, respectively (Fig. 2b and c, and 2d). When the pH decrease from approximately 11 to 3, the SCNs of montmorillonite, illite, and kaolinite decrease by 74.7%, 86.3%, and 93.3%, respectively (Fig. 3).

### Effects of pH on the SCNs of different soils

The changes in the SCNs of the 9 soils with respect to pH are shown in Fig. 4. The repeated experiments have also been carried out (Fig. S2). As the pH decreases, a gradual decline in the SCN is observed across all soil types. In terms of SCNs at varying pH values, the order of the soils is as follows: chernozem > black soil > chestnut soil  $\approx$  yellow-brown soil > dark brown soil > brown soil > red soil > yellow soil > latosol (Fig. 4a and b). For example, at pH approximately 11, the SCN of chernozem is  $-60.2$  cmol/kg, while the SCNs of the black soil, chestnut soil, yellow-brown soil, dark brown soil, brown soil, red soil, yellow soil, and latosol are  $-38.4$ ,  $-25.3$ ,  $-25.1$ ,  $-19.2$ ,  $-14.4$ ,  $-14.5$ ,  $-11.3$ , and  $-10.9$  cmol/kg, respectively (Fig. 4a and b). When the pH decreases from approximately 11 to 4, the SCNs of the black soil, chernozem, chestnut soil, dark brown soil, brown soil, yellow-brown soil, yellow soil, red soil, and latosol decrease by 75.8%, 83.4%, 60.8%, 69.0%, 59.2%, 63.4%, 50.3%, 65.8%, and 79.6%, respectively (Fig. 5).

### X-ray diffraction analysis of 9 soil clays

XRD analysis of diverse soil clays reveal the characteristic diffraction peaks that offer insights into their mineral compositions. The peaks observed at 14.2 and 10.1 Å suggest the presence of vermiculite. Similarly, the peaks at 10.1, 5.12, and 3.30 Å indicate the presence of illite, while the superposition of the peaks at 4.48 Å reveal a combination of illite and montmorillonite. The appearance of peaks at 7.2, 3.56, 2.56, and 2.50 Å indicate the presence of kaolinite. Furthermore, diffraction peaks at 4.23 and 3.30 Å are indicative of quartz (Fig. S3). In specific soil types, such as yellow-brown soil, yellow soil, red soil, and latosol, peaks at 2.69 and 2.42 Å indicate the presence of goethite and hematite, respectively. In latosol, a peak at 4.82 Å signify the presence of gibbsite (Fig. S3).

The types and relative contents of clay minerals in the 9 soil clays are listed in Table 2. Regarding the mineral compositions of the soil clays, the black soil, chernozem, chestnut soil, dark brown soil, brown soil, and yellow-brown soil are composed primarily of 2:1 phyllosilicate, with illite contents exceeding 50% (except for the yellow-brown soil). Additionally, minerals such as vermiculite, kaolinite, and quartz are also present. However, compared to the black soil, chernozem, chestnut soil, dark brown soil, and brown soil, the yellow-brown soil contain higher contents of goethite and hematite. In addition, the yellow soil, red soil, and latosol are composed mainly of kaolinite and oxide minerals (Table 2).

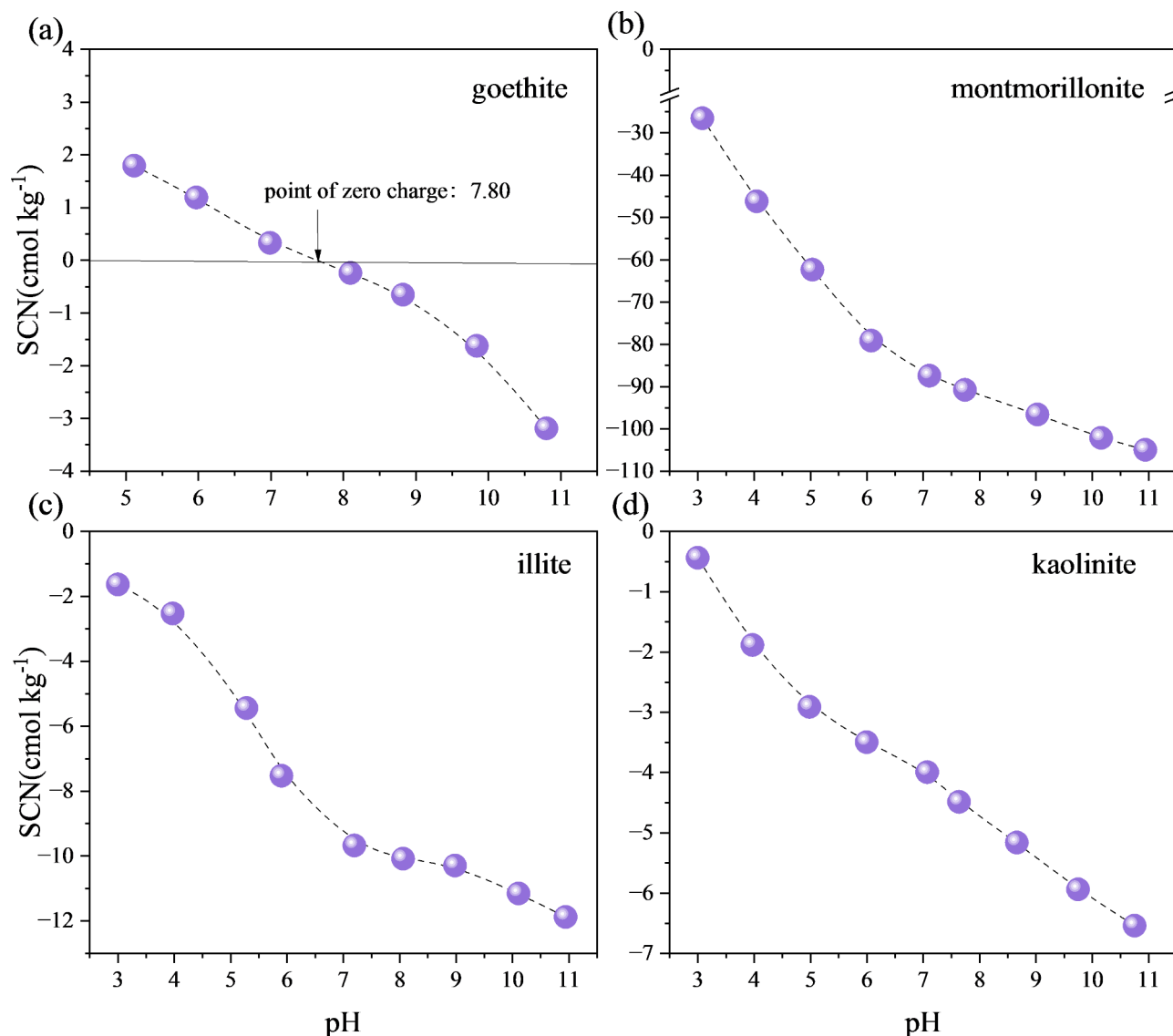


**Fig. 2.** SCNs of (a) goethite, (b) montmorillonite, (c) illite, and (d) kaolinite as functions of pH.

## Discussion

The negative surface charges of goethite, a typical iron oxide found in variably charged soils, notably decreases as the pH decreases. Specifically, when the pH decreases from 10.9 to approximately 7.80, the negative charges of goethite decrease significantly from 3.19 to 0 cmol/kg. This finding aligns remarkably well with the point of zero charge reported in the literature<sup>26,27</sup>, thereby validating the accuracy and reliability of the universal determination method of SCN.

Montmorillonite and illite are the most common silicate clay minerals in soils. Their crystal structures are composed of a layer of Al-O octahedron sandwiched between two layers of Si-O tetrahedron<sup>28</sup>; hence, they are called 2:1 clay minerals. The excess negative charges generated by isomorphous substitution can yield a strong electric field strength of  $10^8$ – $10^{10}$  V/m near the clay particle surface<sup>1</sup>. In such a strong electric field, orbital asymmetric hybridization of surface O atoms occurs on the siloxane surface<sup>21</sup>. Covalent bonds between surface O atoms and adsorbed ions form easily because of the significant changes in the energy of their outer shell orbitals<sup>19</sup>. Li et al.<sup>21</sup> further revealed that the activity of the lone pair electrons in the outer shell orbitals of surface O atoms in the electric field increased linearly with increasing electric field strength based on the quantum mechanical effect of the asymmetric hybridization of atomic orbitals. It indicated that the energy of the outer shell orbital  $\phi_{(1)} = \frac{1}{\sqrt{2}} [\psi_{2s} + \psi_{2p_z(-)}]$  of the surface O atoms of clay minerals increased from the classical orbital energy of  $E_{20}$  to  $E_{20} + 3e\xi \frac{a_0}{(1-a)Z}$ , which was an increase of  $3e\xi \frac{a_0}{(1-a)Z} = 0.4878e\xi a_0$ . In addition, the 1s orbital of H<sup>+</sup> is empty, enabling it to accept activated lone pair electrons from the surface O atoms of clay minerals. These results suggest that in a strong electric field, coordinate/covalent bonds may form between the surface O atoms and H<sup>+</sup>. The chemical bond can be called polarization-induced covalent bonding and may occur in the asymmetric electric field at the clay minerals surface. These coordinate/covalent bonds

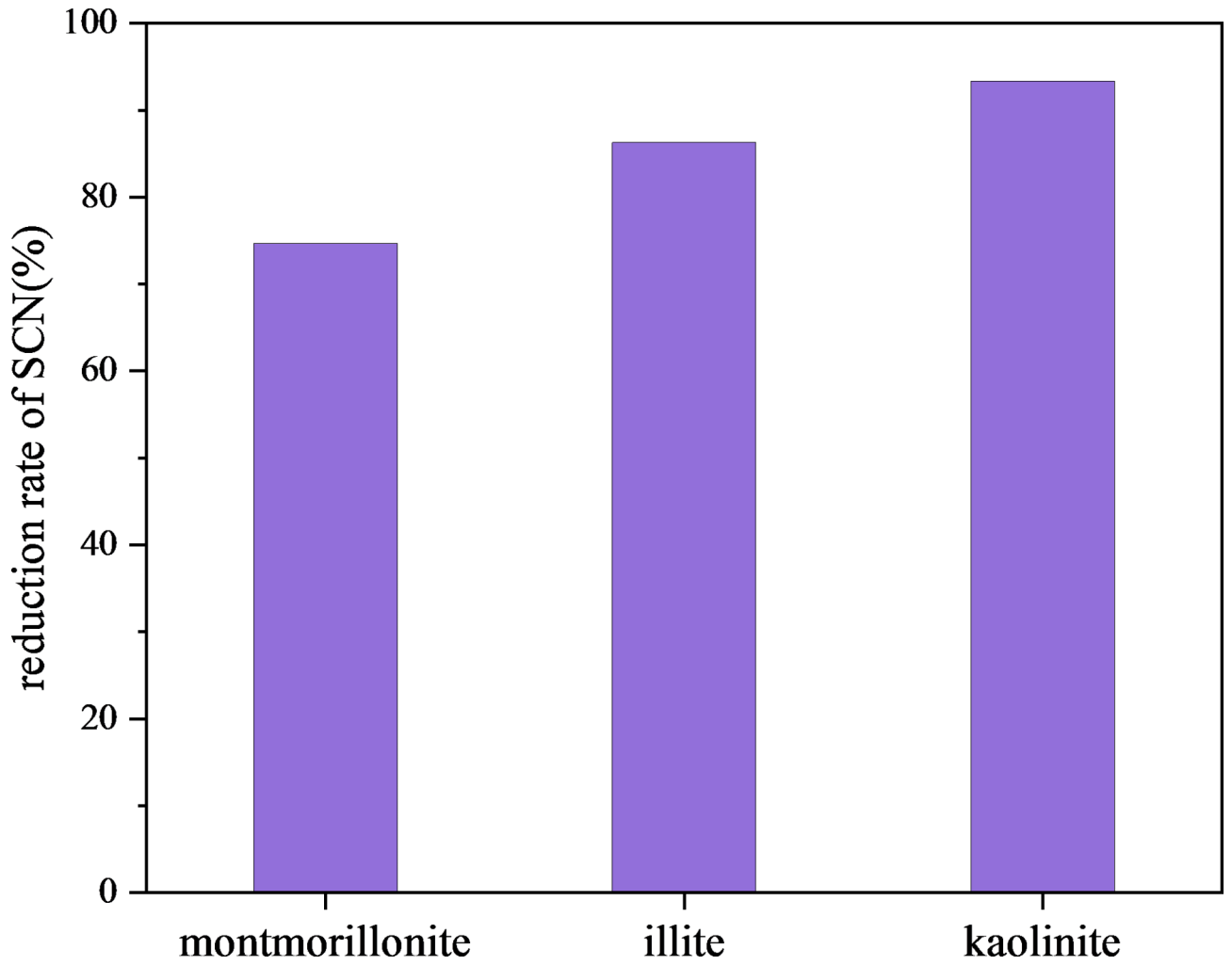


**Fig. 3.** The reduction rates of the SCNs of montmorillonite, illite, and kaolinite when the pH decreases from approximately 11 to 3.

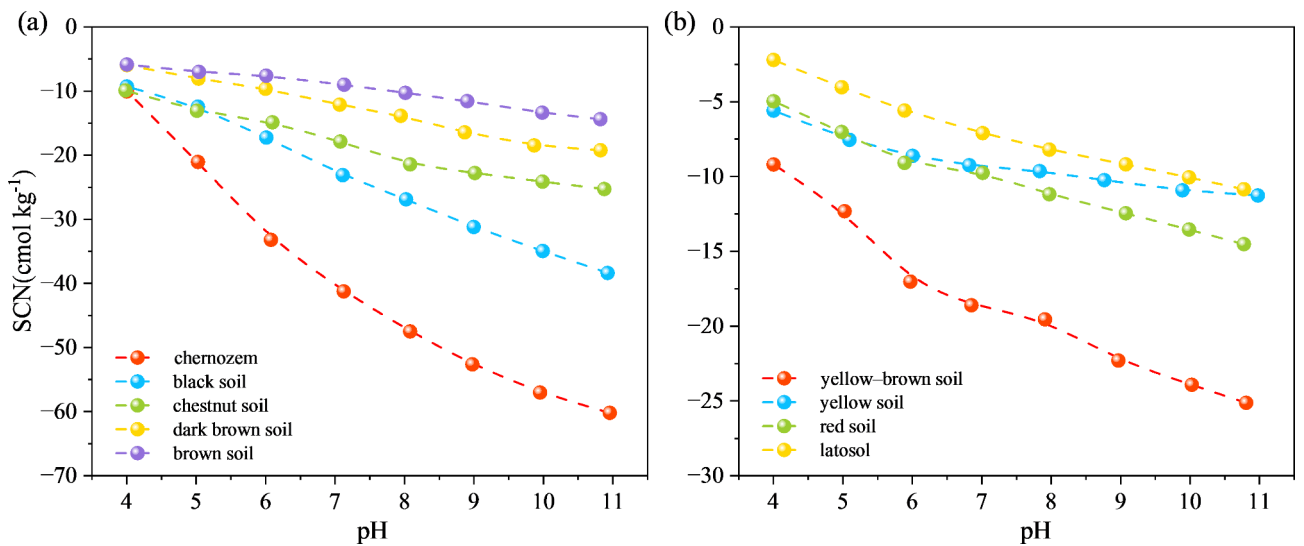


**Fig. 4.** SCNs of (a) permanently charged soils (black soil, chernozem, chestnut soil, dark brown soil, and brown soil) and (b) variably charged soils (yellow-brown soil, yellow soil, red soil, and latosol) as functions of pH.

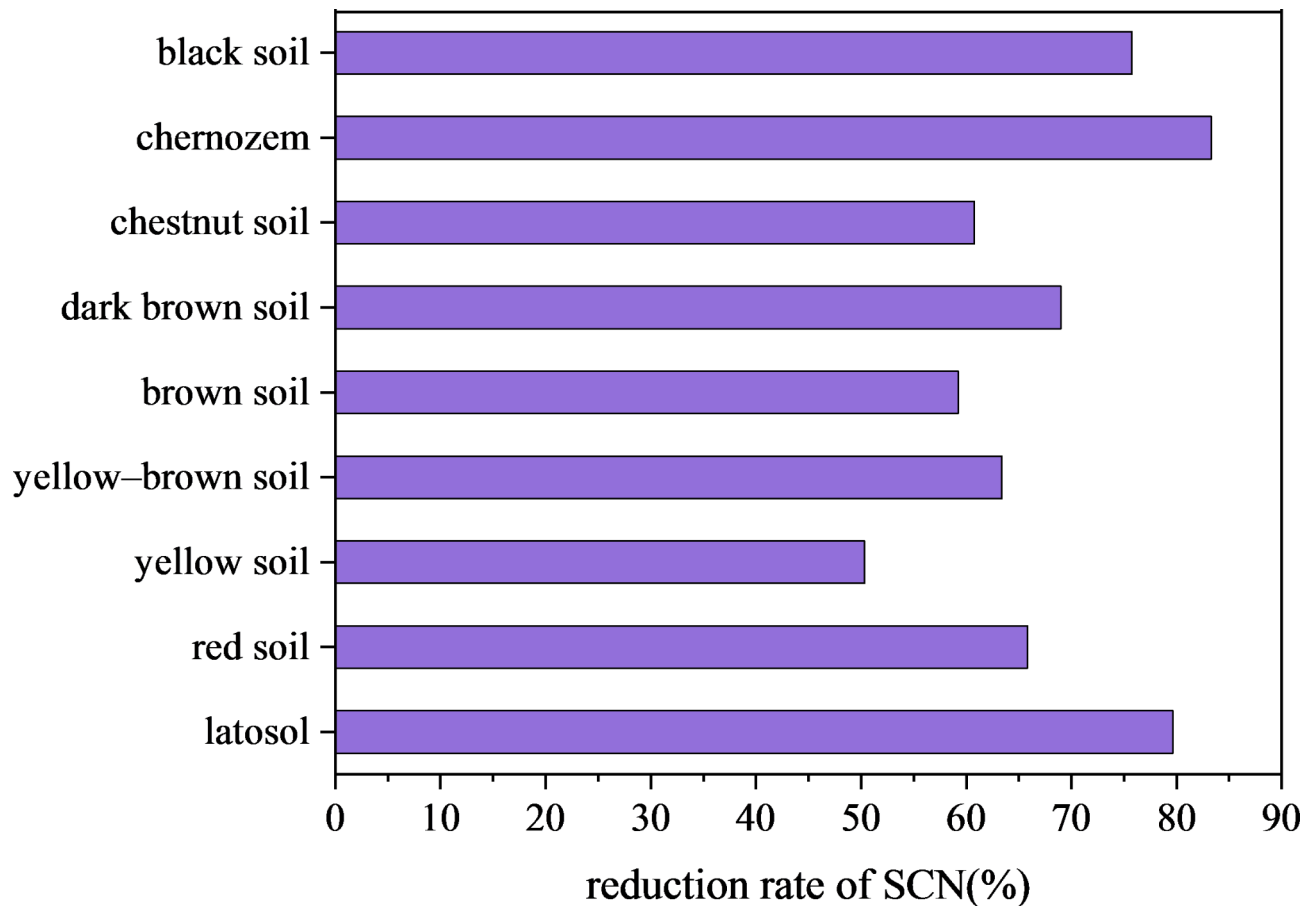


**Fig. 5.** The reduction rates of the SCNs of the permanently/variably charged soils when the pH decreases from approximately 11 to 4.

Soil type		Illite	Montmorillonite	Vermiculite	Quartz	Kaolinite	Goethite	Hematite	Gibbsite
Permanently charged soils	Black soil	62.9	14.7	5.99	5.00	11.4	–	–	–
	Chernozem	68.6	17.2	3.83	4.97	5.45	–	–	–
	Chestnut soil	59.8	22.9	2.90	4.84	9.53	–	–	–
	Dark brown soil	54.7	15.9	8.04	4.85	16.5	–	–	–
	Brown soil	50.1	17.6	6.81	2.94	22.5	–	–	–
Variably charged soils	Yellow-brown soil	36.9	18.7	4.56	2.77	22.7	10.0	4.29	–
	Yellow soil	28.7	6.25	5.58	6.56	34.4	13.7	4.71	–
	Red soil	17.4	3.26	2.87	2.39	31.9	22.9	19.3	–
	Latosol	16.6	1.41	0.69	1.76	45.0	16.5	15.2	3.41

**Table 2.** Types and relative contents of clay minerals in 9 soil clays (%). Note: “–” indicates not detected.

will disappear with the elimination of the electric field<sup>6</sup>. The results of the above experiments show that the SCN of kaolinite, a 1:1 clay mineral, decreased by 93.3% when the pH decreases from approximately 11 to 3, which reflect the variable charge property of kaolinite (Fig. 2d). However, even for the permanently charged montmorillonite and illite, the SCNs also decrease when the pH decreases from approximately 11 to 3 (Fig. 2b and c). The SCNs of montmorillonite and illite decrease by 66.3% and 86.3%, respectively (Fig. 3). Apparently, the polarization-induced covalent adsorption of H<sup>+</sup> on clay mineral surfaces can significantly reduce the SCN.

Compared with those of variably charged minerals, the SCN of montmorillonite exhibit a less pronounced decrease with decreasing pH, whereas the SCN of illite decrease to nearly the same extent as those of variably charged minerals, indicating that robust polarization-induced covalent bonding form between the surface O atoms of illite and H<sup>+</sup> (Fig. 2b, c, and 2d). The nonelectrostatic adsorption energy of H<sup>+</sup> derives from the polarization-induced covalent bonding between H<sup>+</sup> and the surface O atom. The strength of the bonding depends on the energy of the lone pair electrons of the surface O atoms, which is influenced by the electric

field strength<sup>6</sup>. The negative surface charges of montmorillonite are derived mainly from the substitution of aluminum in the Al-O octahedra by Mg<sup>2+</sup>, with each substitution yielding a negative charge. Conversely, the negative surface charges of illite are predominantly a result of the substitution of a fraction of silicon in the silica-oxygen tetrahedra by Al<sup>3+</sup><sup>29</sup>. The electric field generated by these two sources of negative charges on the siloxane surface differ significantly. The permanent negative charges stemming from isomorphic substitution in the Si-O tetrahedron are positioned closer to the siloxane surface, increasing the electric field strength<sup>19</sup>. In contrast, the negative charges generated by isomorphic substitution in the Al-O octahedron are further away from the siloxane surface, resulting in a relatively weak electric field strength. As a result, compared with those of montmorillonite, the surface O atoms of illite exhibit greater covalent activity<sup>19</sup>, leading to more intense polarization-induced covalent interactions<sup>30</sup>.

This method can measure permanent or variable charges at the same time, so the net charges are obtained by an experiment. The charges carried by organic matter are variable, so the SCNs obtained by this method contain the contribution of organic matter. The decreases in SCNs with pH in the permanently charged soils are comparable to or even greater than those observed in the variably charged soils (Figs. 4 and 5). The permanently charged soils (black soil, chernozem and chestnut soil) contain a large amount of organic matter, which is one of the reasons why the SCNs of permanently charged soils are related to pH. The changes in the SCNs with pH is also attributed to 2:1 clay minerals in the soil clay composition, with the combined relative contents of illite, montmorillonite, and vermiculite exceeding 60% (Table 2). The polarization-induced covalent adsorption of H<sup>+</sup> on the clay mineral surface results in a decrease in the negative surface charges. Notably, the lower the pH is, the more significant the decrease in the negative surface charges becomes. However, the contents of organic matter in other permanently charged soils (dark brown soil and brown soil) are less than 2% (Table 1). In addition, the increase of 1% humus in soil colloid leads to an increase of about 1 cmol/kg negative charges<sup>4</sup>, which indicate that the contribution of organic matter to the SCNs of these soils is limited. So the main reason for the changes of their SCNs with pH are polarization induced covalent interactions. For variably charged soils (yellow soil, red soil and latosol), the changes of SCNs with pH are mainly attributed to the iron and aluminum oxides contained.

## Conclusion

In this study, the changes in the SCNs of permanently/variably charged soils and clay minerals with pH were determined by the universal determination method of SCN. The results show that the SCNs of permanently/variably charged soils and clay minerals decrease with decreasing pH. For permanently charged soils with relatively high organic matter content or clay minerals, a decrease in pH promotes the polarization-induced covalent adsorption of H<sup>+</sup> on clay mineral surface, resulting in a decrease in SCN. For permanently charged soils with relatively low organic matter content, however, both the polarization-induced covalent interactions and organic matter are the main cause for the decrease in SCNs with decreasing pH. It follows that the reliability of the concepts of “permanently charged colloid” or “permanently charged soil” are questionable.

The method used in this study to determine the surface charge of clay minerals and soils at different pH provides a new insight for the research on soil and clay minerals. Particularly, it will be useful in early warning or improvement of acidified soils. In addition, it is expected to evaluate the surface properties of other materials at different environmental pH values by this method.

## Data availability

The data that support the findings of this study are available from the corresponding author upon reasonable request.

Received: 4 July 2024; Accepted: 26 September 2024

Published online: 05 October 2024

## References

- Li, H. *et al.* Combined determination of specific surface area and surface charge properties of charged particles from a single experiment. *Soil Sci. Soc. Am. J.* **75**, 2128–2135 (2011).
- Liu, X., Li, H., Li, R., Tian, R. & Hou, J. A new model for cation exchange equilibrium considering the electrostatic field of charged particles. *J. Soils Sediments* **12**, 1019–1029 (2012).
- Ma, R., Hu, F., Liu, J. & Zhao, S. Evaluating the effect of soil internal forces on the stability of natural soil aggregates during vegetation restoration. *J. Soils Sediments* **21**, 3034–3043 (2021).
- Chemistry of Variable Charge Soils*. (Oxford University Press, New York, 1997). <https://doi.org/10.1093/oso/9780195097450.001.0001>.
- Liu, D., Du, W., Liu, X., Tian, R. & Li, H. To distinguish electrostatic, coordination bond, nonclassical polarization, and dispersion forces on cation–clay interactions. *J. Phys. Chem. C* **123**, 2157–2164 (2019).
- Liu, D. *et al.* Polarisation-induced covalent interactions between H<sup>+</sup> and surface O atoms promote clay aggregation. *Eur. J. Soil Sci.* **73**, e13286 (2022).
- Jiang, X., Ma, Y., Yuan, J., Wright, A. L. & Li, H. Soil particle surface electrochemical property effects on abundance of ammonia-oxidizing bacteria and ammonia-oxidizing archaea, NH<sub>4</sub><sup>+</sup> activity, and net nitrification in an acid soil. *Soil Biol. Biochem.* **43**, 2215–2221 (2011).
- Edwards, P., Kochenderfer, J., Coble, D. & Adams, M. Soil leachate responses during 10 years of induced whole-watershed acidification. *Water. Air. Soil Pollut.* **140**, 99–118 (2002).
- Osman, M., Moor, C., Caseri, W. & Suter, U. Alkali metals ion exchange on muscovite mica. *J. Colloid Interface Sci.* **209**, 232–239 (1999).
- Jarosz, R., Szerement, J., Gondek, K. & Mierzwa-Hersztek, M. The use of zeolites as an addition to fertilisers – a review. *Catena* **213**, 106125 (2022).
- Liu, X. *et al.* Asymmetric response of transition metal cationic orbitals to applied electric field. *J. Hazard. Mater.* **468**, 133718 (2024).
- Osuna, F. J., Pavón, E. & Alba, M. D. Design swelling micas: Insights on heavy metals cation exchange reaction. *Appl. Clay Sci.* **182**, 105298 (2019).

13. Confalonieri, G. *et al.* Ion exchange capacity of synthetic zeolite L: a promising way for cerium recovery. *Environ. Sci. Pollut. Res.* **29**, 65176–65184 (2022).
14. Schofield, R. Effect of pH on electric charges carried by clay particles. *J. Soil Sci.* **1**, 3–8 (1949).
15. Xu, R., Zhao, A. & Ji, G. Effect of low-molecular-weight organic anions on surface charge of variable charge soils. *J. Colloid Interface Sci.* **264**, 322–326 (2003).
16. Liu, D., Tian, R., Liu, X. & Li, H. Polarization induced covalent/hydrogen bonding adsorption of NH<sub>4</sub><sup>+</sup> and K<sup>+</sup> in soils: Comparison study on permanently and variably charged soils. *J. Soils Sediments* **24**, 722–731 (2024).
17. Yu, Z. *et al.* Importance of soil interparticle forces and organic matter for aggregate stability in a temperate soil and a subtropical soil. *Geoderma* **362**, 114088 (2020).
18. Wen, X. *et al.* Surface charge properties of variable charge soils influenced by environmental factors. *Appl. Clay Sci.* **189**, 105522 (2020).
19. Sposito, G. *The Surface Chemistry of Soils*. Spenter Inc (Oxford University Press, New York, 1984).
20. Stumm, W. *Chemistry of the Solid-Water Interface*. (Chemistry of the Solid-Water Interface, 1992).
21. Li, Q., Yang, S., Tang, Y., Yang, G. & Li, H. Asymmetric hybridization orbitals at the charged interface initiates new surface reactions: a quantum mechanics exploration. *J. Phys. Chem. C* **123**, 25278–25285 (2019).
22. Li, Q., Liu, X. & Shi, W. Orbital asymmetric hybridization enhances surface lewis acid-base reactions of charged clay catalysts. *Appl. Surf. Sci.* **575**, 151731 (2022).
23. Atkinson, R., Posner, A. & Quirk, J. Adsorption of potential-determining ions at ferric oxide-aqueous electrolyte interface. *J. Phys. Chem.* **71**, 550–558 (1967).
24. Toraya, H. A new method for quantitative phase analysis using X-ray powder diffraction: Direct derivation of weight fractions from observed integrated intensities and chemical compositions of individual phases. *J. Appl. Crystallogr.* **49**, 1508–1516 (2016).
25. Liu, X., Li, H., Li, R., Tian, R. & Xu, C. Combined determination of surface properties of nano-colloidal particles through ion selective electrodes with potentiometer. *Analyst* **138**, 1122–1129 (2013).
26. Hiemstra, T., De Wit, J. C. M. & Van Riemsdijk, W. H. Multisite proton adsorption modeling at the solid/solution interface of (hydr)oxides: A new approach. *J. Colloid Interface Sci.* **133**, 105–117 (1989).
27. Kosmulski, M. The pH dependent surface charging and points of zero charge. VIII. Update. *Adv. Colloid Interface Sci.* **275**, 102064 (2020).
28. Cui, J., Zhang, Z. & Han, F. Effects of pH on the gel properties of montmorillonite, palygorskite and montmorillonite-palygorskite composite clay. *Appl. Clay Sci.* **190**, 105543 (2020).
29. Rudmin, M. *et al.* Origin of fe-rich clay minerals in early devonian volcanic rocks of the northern minusa basin, eastern siberia. *Appl. Clay Sci.* **241**, 107014 (2023).
30. Avena, M. J. & De Pauli, C. P. Proton adsorption and electrokinetics of an argentinean montmorillonite. *J. Colloid Interface Sci.* **202**, 195–204 (1998).

## Acknowledgements

This work was supported by the National Key R&D Program of China (2023YFD1900300).

## Author contributions

H.C: Conceptualization, methodology, data curation, writing—original draft, formal analysis, writing—review and editing, and visualization. X.L: Conceptualization, methodology, and formal analysis. B.F: Methodology, review, and editing. J.S: Validation and methodology. D.M: Validation and methodology. X.C: Validation and methodology. H.L: Conceptualization, methodology, writing—original draft, writing—review and editing, formal analysis, visualization, funding acquisition, and project administration.

## Competing interests

The authors declare no competing interests.

## Additional information

**Supplementary Information** The online version contains supplementary material available at <https://doi.org/10.1038/s41598-024-74563-6>.

**Correspondence** and requests for materials should be addressed to H.L.

**Reprints and permissions information** is available at [www.nature.com/reprints](http://www.nature.com/reprints).

**Publisher's note** Springer Nature remains neutral with regard to jurisdictional claims in published maps and institutional affiliations.

**Open Access** This article is licensed under a Creative Commons Attribution-NonCommercial-NoDerivatives 4.0 International License, which permits any non-commercial use, sharing, distribution and reproduction in any medium or format, as long as you give appropriate credit to the original author(s) and the source, provide a link to the Creative Commons licence, and indicate if you modified the licensed material. You do not have permission under this licence to share adapted material derived from this article or parts of it. The images or other third party material in this article are included in the article's Creative Commons licence, unless indicated otherwise in a credit line to the material. If material is not included in the article's Creative Commons licence and your intended use is not permitted by statutory regulation or exceeds the permitted use, you will need to obtain permission directly from the copyright holder. To view a copy of this licence, visit <http://creativecommons.org/licenses/by-nc-nd/4.0/>.

© The Author(s) 2024